ELSEVIER

Nuclear Instruments and Methods in Physics Research A 463 (2001) 387–392

NUCLEAR INSTRUMENTS & METHODS IN PHYSICS RESEARCH Section A

www.elsevier.nl/locate/nima

Observation of coherent synchrotron radiation from the NSLS VUV ring

G.L. Carr[a,*], S.L. Kramer[a], J.B. Murphy[a], R.P.S.M. Lobo[b], D.B. Tanner[b]

[a] *National Synchrotron Light Source, Brookhaven National Laboratory, Upton, NY 11973, USA*
[b] *Department of Physics, University of Florida, Gainesville, FL 32611, USA*

Received 20 October 2000; received in revised form 3 January 2001; accepted 7 January 2001

Abstract

We report the observation of multiparticle coherent emission in the very far infrared from bunched electrons in an electron storage ring. The emission occurs in quasi-periodic bursts, and only when the electron beam current exceeds a threshold value, suggesting an instability-driven modulation of the electron bunch density. For the operating conditions reported, the spectral content of the coherent emission is peaked near a wavelength of 7 mm. This wavelength is much shorter than the nominal electron bunch length, indicating the presence of a density modulation within the bunch.

PACS: 29.27.Bd; 29.20.Dh; 41.60.Ap

Keywords: Coherent emission; Synchrotron radiation; Far-infrared source

1. Introduction

Synchrotron radiation is produced when electron bunches traverse the magnetic guide field of a storage ring. So long as the size of the bunch (which generally contains of order 10^{10}–10^{12} electrons) is larger than the wavelength, the radiation from these bunches is incoherent: the total radiated intensity is the sum of the radiated intensities of the individual electrons. At long wavelengths, in contrast, the electric fields generated by each electron superimpose coherently, making the intensity much larger than the sum of the individual intensities. In this article we report the observation of coherent far-infrared synchrotron radiation at wavelengths much shorter than the bunch length. Characteristics of the radiation indicate it results from a longitudinal instability of the electron bunch. Instabilities of this type are of great concern for light sources that rely on extremely short-duration electron bunches. On the other hand, coherent emission from electron storage rings may become a valuable source for millimeter wave spectroscopy.

The radiation intensity produced by multiple identical particles in a bunch emitting synchrotron radiation can be written as [1,2]

$$\frac{\mathrm{d}I}{\mathrm{d}\omega_{\text{multiparticle}}} = [N + N(N-1)f(\omega)]\frac{\mathrm{d}I}{\mathrm{d}\omega_{\text{oneparticle}}} \equiv P(\omega)_{\text{incoherent}} + P(\omega)_{\text{coherent}} \quad (1)$$

*Corresponding author. Tel.: +1-631-344-2237; fax: +1-631-344-3238.
E-mail address: carr@bnl.gov (G.L. Carr).

0168-9002/01/$ - see front matter © 2001 Published by Elsevier Science B.V.
PII: S0168-9002(01)00521-6

where N is the number of particles in the bunch, $dI/d\omega_{oneparticle}$ is the far-field intensity per spectral bandwidth produced by a single particle and

$$f(\omega) = \left| \int_{-\infty}^{\infty} e^{i\omega\hat{n}\cdot z/c} S(z)\, dz \right|^2 \quad (2)$$

is the Fourier transform of the (normalized) longitudinal electron density $S(z)$. For spectral ranges where $f(\omega)$ is effectively zero, Eq. (1) gives an intensity that scales linearly with the number of particles. This is standard incoherent synchrotron radiation emission. But for spectral ranges where $f(\omega)$ is not zero, $dI/d\omega$ has a *coherent* term that scales as N^2. Since N is typically very large ($\sim 10^{11}$), the coherent part easily dominates over the incoherent term when $f(\omega) > 0$. For a typical electron bunch where the longitudinal density function is Gaussian, the spectral range for coherent emission also has a Gaussian dependence (centered at zero frequency) of width $\sigma_\omega = c/2\pi\sigma_L$ where σ_L is the bunch length. An electron bunch with $\sigma_L = 5\,cm$, therefore, emits coherently for frequencies up to $\sim 1\,GHz$. However, such emission can be difficult to observe [3] since the waveguide cutoff frequency for the storage ring's metallic vacuum chamber is typically around 10 GHz. If the electron bunch is short enough (i.e., $\leqslant 10\,ps$ duration), or a short period modulation of the bunch density can be imposed, coherent emission at observable frequencies can occur. From Eq. (1), the ratio of the coherent to incoherent radiated intensity is

$$\frac{P(\omega)_{coherent}}{P(\omega)_{incoherent}} \cong Nf(\omega) \quad (3)$$

so that a measure of this ratio can be used to extract information on the longitudinal particle density function through Eq. (2) (the precise density can not be determined without phase information). This effect has been previously observed and utilized in linac-driven systems [4–6].

In addition to intentional modifications of the electron bunch, instabilities can lead to variations in the bunch shape and density, which in turn may lead to coherent emission. This paper presents evidence for the emission of coherent synchrotron radiation from the NSLS VUV ring. The radiation occurs in less than 1 ms duration bursts at millimeter wavelengths; much shorter than the nominal electron bunch length of $\sigma_L \sim 5\,cm$. This and other evidence suggest that the emission is a consequence of micro-bunching (a density modulation within a bunch) that is characteristic of the microwave instability [7]. The details of this emission process are of interest both as a potential source of electromagnetic radiation and its relevance to the operation of high-energy accelerators and short wavelength FELs.

2. Experimental details

Our measurements were conducted using the VUV ring at the National Synchrotron Light Source (NSLS/BNL). This storage ring has a double-bend achromat lattice with four superperiods and operates as a dedicated synchrotron radiation source. The bending radius is 1.91 m in each of the eight dipole magnets. The RF accelerating system operates at 52.9 MHz and the ring orbit frequency is 5.9 MHz. Though the ring energy can be varied from below 500 MeV up to 800 MeV, we conducted most of our studies at the injection energy of 737 MeV. A single bunch of electrons was used for all of our measurements to avoid any complications stemming from coupled-bunch dynamics. The ring supports up to 400 mA beam current (average value) in one-bunch mode, corresponding to 4×10^{11} electrons. Because we do not have accurate bunch length measurements for all conditions, we report average current values rather than peak currents. The lattice used for normal operations as a synchrotron radiation source (i.e., dispersion-free straight sections for insertion devices) has a momentum compaction $\alpha_0 = 0.0235$ and yields a synchrotron tune near 11.7 kHz. Modifying the ring lattice allows the momentum compaction to be varied by more than two orders of magnitude, including both positive and negative values [8].

The presence of short wavelength coherent emission is detected at beamline U12IR [9]. This beamline extracts dipole bending magnet radiation through a 6 cm square aperture (90×90 mrad of collection angle), which is comparable to the interior dimension of the storage ring vacuum

chamber. Mirror and waveguide optics transport the long-wavelength infrared to a lamellar grating interferometer [10] and ℓHe cooled bolometric detector. The longest detectable wavelength for this system is ~ 10 mm (frequency of $1\,\mathrm{cm}^{-1}$ or 30 GHz). The short wavelength limit is about 100 μm, determined by filters. The detector has a thermal time constant of about 200 μs.

3. Results

During normal operations of the VUV ring, the far IR power is temporally smooth on time scales longer than the detector response time (i.e., we do not detect the passage of individual electron bunches). The power varies linearly with beam current per bunch up to a certain threshold, above which bursts of radiation are emitted [11]. An example of these bursts is shown in Fig. 1. The time structure is rather complex, and (along with the beam current threshold value) varies with operating conditions. Typically, bursts occur with varying amplitude, and at time intervals ranging from ~ 1–~ 10 ms (increasing to >1 s when the beam current is close to threshold). The signal rise time provides a measure of the burst duration down to the detector's amplifier limit of ~ 1 μs. For $\alpha = \alpha_0$ (the normal momentum compaction), the signal rise time is found to be a few tens of microseconds. As the current is increased beyond the threshold value, the magnitude of a typical burst also increases. We measured the time-averaged power output as a function of beam current for the nominal momentum compaction α_0, with the results shown in Fig. 2. The average power first increases linearly with beam current, as expected for normal incoherent emission. When the current exceeds the threshold value ($I > I_{\mathrm{th}} = 100$ mA for this set of conditions), emission bursts appear. At this point, the average power increases at a rate greater than linear, tending toward the square of the *excess* beam current [i.e., as $(I - I_{\mathrm{th}})^2$].

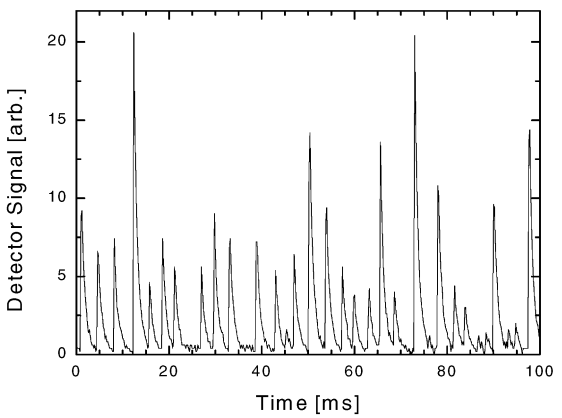

Fig. 1. Far infrared detector output versus time showing emission bursts for $I > I_{\mathrm{th}}$.

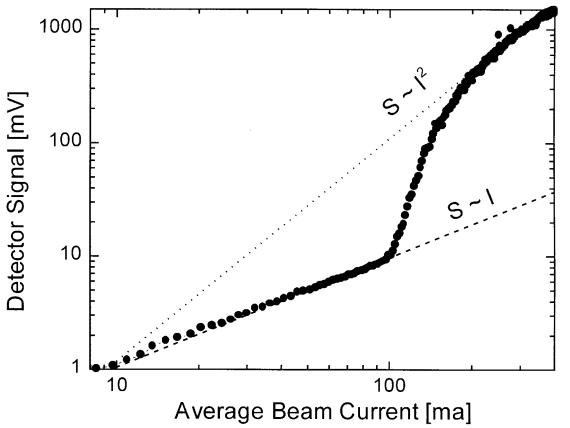

Fig. 2. Measured output power versus average beam current in a single bunch, showing the onset of coherent emission at $I_{\mathrm{th}} = 100$ mA where the dependence of signal S on current I begins its changeover from I to I^2.

We measured the spectral content of both the coherent and incoherent emission using the U12IR lamellar grating interferometer. Results for each are shown in Fig. 3. The sampling time for each point was a few seconds, thus the coherent spectrum represents the time-average over many bursts. Note that both the coherent and incoherent signals show considerable spectral structure due to the propagation of light inside the storage ring dipole vacuum chamber.[1] Despite this structure, we were able to calculate a ratio, thus eliminating most of the spectral characteristics associated with

[1] This structure is due to interference between the directly observed source and an upstream image, reflected from the outer wall of the dipole chamber [12].

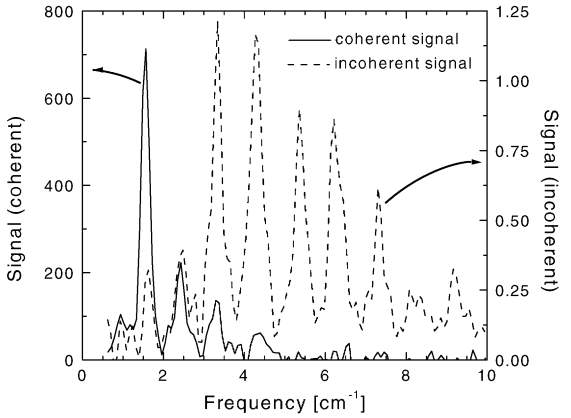

Fig. 3. Spectral signal for both incoherent (dashed line, right axis) and coherent (solid line, left axis) synchrotron radiation emission. The complex structure of both spectra is due to interference between two source points, the second from an upstream tangent point reflected in the outer wall of the storage ring chamber.

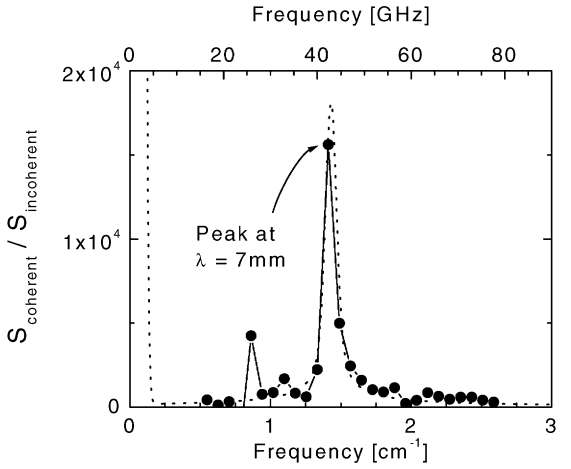

Fig. 4. (Symbols and solid line): measured spectral content of the coherent emission, relative to the incoherent synchrotron spectrum (ratio of spectra shown in Fig. 3). The small peak near $0.8\,\mathrm{cm}^{-1}$ is probably due to poor S/N for the incoherent spectrum. Dotted line: modeled spectral content, including a non-observable Gaussian component, centered at zero frequency, for the overall bunch shape.

the spectrometer and beamline, as well as the intrinsic content of incoherent synchrotron radiation. The result, shown in Fig. 4, is peaked at approximately 7 mm wavelength (42 GHz). This spectral content can be used to estimate the

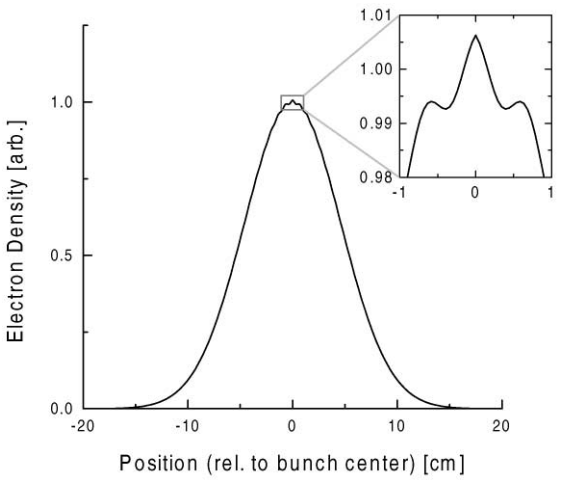

Fig. 5. Real Fourier transform of the modeled spectral content of Fig. 3. The relative phase of the modulation (with respect to the overall bunch envelope) is unknown, but was assumed to be symmetric for the calculation.

electron bunch profile by means of Eq. (2). To facilitate the analysis, we modeled the observed spectral content plus a Gaussian to account for the (non-observable) coherent emission from the overall electron bunch profile. The model function is also shown in Fig. 4, along with the actual spectral content. A Fourier transform then yields a plausible electron-bunch density function, shown in Fig. 5. Note that we cannot determine a precise density profile due to a lack of phase information. In addition, the relative magnitude of the bunch modulation is only a rough order-of-magnitude estimate because it occurs in bursts that vary with the amount of current over threshold and other operating parameters. Lastly, we should note that the spectral content reported here was observed for one particular set of operating conditions. More recent measurements suggest the spectral content is variable, depending on parameters such as the amount the beam current is above threshold.

4. Discussion

The wavelength of the emission bursts and the unusual time-structure suggest a process related to

the so-called microwave instability [7]. This particular type of longitudinal instability results when electrons interact with each other through a short-range wake field. The strength of this interaction is characterized by a complex, broad-band impedance determined by the materials and dimensions of the beampipe, RF cavities, and other structures such as beam ports and bellows. The threshold condition for this instability has been given by a number of authors. For unbunched (coasting) beams, the Keil–Schnell criterion for stability [13] gives

$$eI\frac{Z_n}{n} \leqslant 2\pi\alpha E\sigma_E^2 \quad (4)$$

where I is the average beam current, Z_n is the impedance for disturbance with mode number n, α is the momentum compaction, E is the electron energy and σ_E is the normalized energy spread. For constant electron energy (and energy spread), Eq. (4) implies a threshold current scaling linearly with momentum compaction, or as the synchrotron frequency f_{s0} squared (the subscript indicates a value in the limit of zero beam current).

$$I_{\rm th} \propto \alpha \propto f_{s0}^2 \quad \text{(unbunched beam)}. \quad (5)$$

For a bunched beam, the current in Eq. 5 can be replaced with its peak value $I_{\rm peak}$ [14]. However, accurate measurements of the beam current are usually a time-average over many orbits ($I_{\rm ave}$), rather than the instantaneous peak value. We therefore, make use of $I_{\rm peak} = I_{\rm ave}S/\sigma_{\rm L}$, where S is bunch separation and $\sigma_{\rm L}$ is the bunch length. Neglecting bunch lengthening due to RF potential well distortion and assuming other parameters are fixed, $\sigma_{\rm L}$ varies as $\alpha^{1/2}$. The resulting threshold current (time average) for a bunched beam becomes

$$I_{\rm th} \propto \alpha^{3/2} \propto f_{s0}^3 \quad \text{(bunched beam)}. \quad (6)$$

We checked for this dependence by measuring the single bunch threshold current while the momentum compaction was varied over a wide range ($-\alpha_0 \leqslant \alpha \leqslant +2\alpha_0$). The ring's energy and RF cavity voltage (either of which affects the electron bunch length) were kept fixed. The measured threshold current behavior is shown in Fig. 6, which gives a log–log plot of $I_{\rm th}$ versus f_{s0} for both positive and negative α. A single power law is not observed but rather a changeover from a cubic to a quadratic dependence as the synchrotron frequency and threshold current increase. This changeover may be due to RF potential well distortion, which increases with beam current and eventually leads to a bunch length that no longer scales like $\alpha^{1/2}$. The results for low threshold current are less susceptible to this effect. Thus the results are consistent with Eq. (6), supporting our notion that the coherent emission results from a longitudinal instability driven by wake-field interactions.

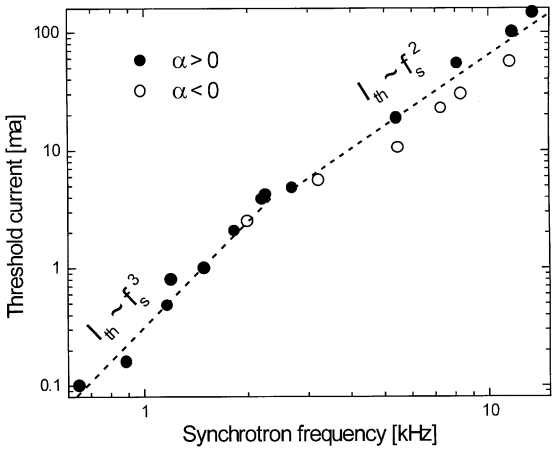

Fig. 6. Measured threshold current (time average) versus synchrotron frequency for both positive (solid circles) and negative (open circles) momentum compaction. The dashed lines indicate $I_{\rm th} \sim f_{s0}^3$ when the synchrotron frequency and $I_{\rm th}$ are small, changing over to $I_{th} \sim f_{s0}^2$ at higher values.

As noted above, the rate at which the instability grows and decays is typically faster than our detector can resolve. However, we did observe longer duration bursts as f_{s0} (i.e., α) was reduced. In particular, for $f_{s0} \sim 1$ kHz the bolometer signal risetime was $>100\,\mu$s. While the detailed rates for the instability to grow and decay were never resolved, we know that the process occurs in less than $200\,\mu$s, which is more than an order of magnitude shorter than the synchrotron damping time (~ 10 ms). Thus, the decay cannot be attributed to synchrotron radiation damping alone. At present we do not understand what determines the time structure of the bursts.

5. Conclusions

In summary, the NSLS VUV ring produces coherent emission with a wavelength of ~ 7 mm. The emission appears in short ($< 100\,\mu$s) duration bursts at intervals of a few milliseconds, but only when the beam current exceeds a threshold value. The dependence of this threshold on momentum compaction is consistent with a longitudinal instability that is driven by wake-field mediated electron–electron interactions. The resulting density modulation of the electron bunch produces coherent emission at millimeter wavelengths. The detailed beam impedance and physical structures leading to this particular instability are not known. We note that our analysis does not include the effects of electron-beam induced potential well distortions to the RF cavity voltage. Such distortions may account for the change over from bunched to "coasting beam" behavior in the dependence of threshold current on synchrotron frequency. Finally, we note that bursts of coherent microwave emission have been observed at SURF II (NIST) [15], apparently due to variations in the entire bunch length. Emission bursts have been observed recently at MAX-II (Lund) [16] and BESSY II [17], but the spectral content (ratio of coherent to incoherent emission) was not reported.

Acknowledgements

We are grateful for assistance from J.D. LaVeigne, G. Ramirez and the NSLS operations staff, plus beneficial conversations with D.H. Reitze (U. Florida), J.-M. Wang, N. Towne, S. Krinsky, and G.P. Williams (NSLS). This work was supported by the U.S. Department of Energy through Contracts DE-AC02-98CH10886 at the NSLS and DE-FG02-96ER45584 at the University of Florida.

References

[1] L.I. Schiff, Rev. Sci. Instrum. 17 (1946) 6.
[2] S. Nodvick, D.S. Saxon, Phys. Rev. 96 (1954) 180.
[3] G.P. Williams, C.J. Hirschmugl, E.M. Kneedler, P.Z. Takacs, M. Shleifer, Y.J. Chabal, F.M. Hoffmann, Phys. Rev. Lett. 62 (1989) 261; C.J. Hirschmugl, M. Sagurton, G.P. Williams, Phys. Rev. A 44 (1991) 1316.
[4] E.B. Blum, U. Happek, A.J. Sievers, Nucl. Instr. and Meth. A 307 (1991) 568.
[5] R. Lai, A.J. Sievers, AIP Conf. Proc. 367 (1996) 312.
[6] T. Nakazato, M. Oyamada, N. Niimura, S. Urasawa, O. Konno, A. Kagaya, R. Kato, T. Kamiyama, Y. Torizuka, T. Nanba, Y. Kondo, Y. Shibata, K. Ishi, T. Ohsaka, M. Ikezawa, Phys. Rev. Lett. 63 (1989) 1245.
[7] J.-M. Wang, C. Pellegrini, BNL 51236, 1979; J.-M. Wang, Phys. Rev. E 58 (1998) 984.
[8] S.L. Kramer, J.B. Murphy, Proceedings of the 1999 Particle Accelerator Conference, IEEE, New York, 1999, p. 140.
[9] R.P.S.M. Lobo, J.D. LaVeigne, D.H. Reitze, D.B. Tanner, G.L. Carr, Rev. Sci. Instrum. 70 (1999) 2899.
[10] R.L. Henry, D.B. Tanner, Infrared Phys. 19 (1979) 163.
[11] G.L. Carr, S.L. Kramer, J.B. Murphy, J. LaVeigne, R.P.S.M. Lobo, D.H. Reitze, D.B. Tanner, Proceedings of the 1999 Particle Accelerator Conference, New York, 1999, p. 134.
[12] G.L. Carr et al, in preparation.
[13] E. Keil, W. Schnell, CERN-ISR-TH-RF/69-48, 1969.
[14] D. Boussard, CERN LABII/RF/INT/75-2, 1975.
[15] A.R. Hight-Walker, U. Arp, G.T. Fraser, T.B. Lucatorto, Proc. SPIE 3153 (1997) 42.
[16] Å. Andersson, M.S. Johnson, B. Nelander, Proc. SPIE 3775 (1999) 77.
[17] M. Abo-Bakr, J. Feikes, K. Holldack, D. Ponwitz, G. Wüstefeld, Proceedings of the 2000 European Particle Accelerator Conference, Vienna, Austria, 2000, p. 720.